Radiation Physics and Chemistry 156 (2019) 222–230

Contents lists available at ScienceDirect

Radiation Physics and Chemistry

journal homepage: www.elsevier.com/locate/radphyschem

Novel method exploration of monitoring neutron beam using Cherenkov photons in BNCT

Diyun Shu[a], Xiaobin Tang[a,b,*], Changran Geng[a], Xudong Zhang[a], Chunhui Gong[a], Wencheng Shao[a], Yuanhao Liu[a,c]

[a] Nanjing University of Aeronautics and Astronautics, Department of Nuclear Science and Engineering, Nanjing 210016, China
[b] Collaborative Innovation Center of Radiation Medicine of Jiangsu Higher Education Institutions, Nanjing 210016, China
[c] Neuboron Medtech Ltd., Nanjing 211112, China

ARTICLE INFO

Keywords:
Cherenkov photons
Boron neutron capture therapy
Neutron beam
Monitoring

ABSTRACT

Ensuring the stability of the neutron beam during boron neutron capture therapy (BNCT) is essential. The goal of this work was to explore a novel method using Cherenkov photons for real-time monitoring of neutron beam in BNCT. The Monte Carlo toolkit Geant4, was used to calculate the Cherenkov photons and dose based on a cubic phantom and Chinese hybrid radiation phantom under different conditions. Based on the study on the cubic phantom, the change of neutron beam characteristics indeed have an impact on dose, which needs quality assurance. The relationship between Cherenkov photons and gamma dose was favorable. The maximum relative variation of the generation of Cherenkov photons is approximately 3.51%, even when the relative change of boron concentration reaching 60%. However, comparing the results of the neutron beam with the original characteristics, the maximum relative variation of Cherenkov photons reaches 14.75% and 14.68% for the usage of Neuboron- spectrum and 5-degree rotation of neutron beam field orientation, respectively. Therefore, the intensity and distribution of Cherenkov photons can only be observably changed by neutron beam characteristics. Based on the Chinese hybrid radiation phantom, the changes in the intensity and distribution of Cherenkov photons can also be observed inside the phantom, and these changes are evident by a detector outside the phantom. Thus, Cherenkov photons has the potential application for neutron beam monitoring.

1. Introduction

Boron neutron capture therapy (BNCT) is a binary-targeted therapy, which needs the combination of neutron beam and boron-delivery agents (Perks et al., 1988; Moss, 2014). Neoplastic cells can be effectively killed through BNCT, whereas the normal cells suffer little harm. In recent years, many countries are developing the accelerator-based BNCT (AB-BNCT) by which the device can be installed in hospitals to widely promote its use in the future (Green, 1998; Blue and Yanch, 2003; Lee et al., 2014). Meanwhile, with the increasing number of patients with cancer treated by BNCT, the quality assurance of BNCT needs to be taken more seriously attention to prevent excess irradiation or poor therapeutic effect.

The purpose of the BNCT quality assurance is to ensure the accuracy of dose received by patients. However, reasonable methods for real-time *in vivo* dose measurement are not yet established. In fact, the BNCT dose is determined by neutron beam characteristics and boron concentration distribution in which accuracy could be guaranteed through the real-time quality assurance of the two aspects together. Some developing methods for the real-time quality assurance of boron distribution were reported (Verbakel and Stecher-Rasmussen, 1997; Probst, 1999; Wittig et al., 2008). The neutron beam characteristics are measured by radiation detector for quality assurance (Tanner et al., 1999; Auterinen et al., 2004). However, a real-time quality assurance method that can directly monitor the stability of the neutron beam delivered to the patient is still lacking.

During the treatment of BNCT, many factors can lead to the inaccuracy of the neutron beam output. The intensity and energy spectrum of neutron beam might be changed by the malfunction or instability of the facility (Raaijmakers et al., 1996). In addition, the set-up error or anatomical change of patient leads to the inaccuracy of the relative position or orientation between neutron beam field and tumor position, which also can be considered as the inaccuracy of neutron beam field orientation (Palmer et al., 2002). Particularly, the uncertainty of neutron beam output further increases after using the intelligent converter and adjustable filter-moderator system, which will

* Corresponding author at: Nanjing University of Aeronautics and Astronautics, Department of Nuclear Science and Engineering, Nanjing 210016, China.
E-mail address: tangxiaobin@nuaa.edu.cn (X. Tang).

https://doi.org/10.1016/j.radphyschem.2018.11.024
Received 3 April 2018; Received in revised form 27 October 2018; Accepted 23 November 2018
Available online 26 November 2018

be used for the intensity and energy spectrum modulation of the beam in the future (Nigg et al., 2002). The malfunction of the system, in addition to human errors in the setup of this system for different patients, are possible during treatment. Thus, exploring a real-time monitoring method of the neutron beam is extremely necessary.

Cherenkov radiation is a kind of optical light which is emitted when a charged particle travels at a speed greater than the phase velocity of light in the medium (Cherenkov, 1934). Recently, several studies were conducted on the usage of Cherenkov radiation for quality assurance in x-ray, electron, and proton radiotherapy, which are attributed to a certain relationship between the number of Cherenkov photons and dose deposition (Silva and Pang, 2012; Helo et al., 2014a, 2014b; Zhang et al., 2014; Shu et al., 2016). Cherenkov radiation can also be generated by secondary-charged particles of gamma rays from the neutron capture reaction in BNCT. The feasibility of Cherenkov radiation for boron concentration measurement has been explored in the previous study. Moreover, a certain correlation between the number of Cherenkov photons and gamma dose may be evident, which enables the real-time monitoring neutron beam through detecting Cherenkov photons in BNCT. Although the penetrability of Cherenkov photon is poor, the Cherenkov photons emitting from superficial tissue can still be utilized to play its role.

In this study, we first constructed a cubic phantom comprising a tumor region. Based on the cubic phantom, BNCT doses with varied neutron beam characteristics were investigated. Then, we explored the distribution of gamma dose and Cherenkov photons under different boron concentrations and neutron beam characteristics, and analyzed the feasibility of neutron beam real-time monitoring using Cherenkov photons. Furthermore, the distributions of Cherenkov photons generated in the phantom and detected by a detector were calculated based on the Chinese hybrid radiation phantom (CHRP) to further confirm the effectiveness of this method in a more realistic situation.

2. Materials and methods

Geant4 Monte Carlo toolkit was used to perform the coupled simulation for neutrons, charged particles, photons, and Cherenkov photons (Agostinelli et al., 2003). The generation and transportation of Cherenkov photons depends on the optical properties of medium, imported into Geant4. Optical properties used in this study were obtained from Bashkatov et al. (2011). Two types of phantoms containing spherical tumors were constructed in Geant4. The first was the cubic phantom, which was used to study the relationships between characteristics of neutron beam and distribution of Cherenkov photons emission. We also employed a Chinese reference radiation phantom to investigate this method in a more realistic situation.

2.1. Phantoms and boron distributions

The size of the tumor-containing cubic phantom consisting of soft tissue was $15 \times 15 \times 15\ cm^3$ (see Fig. 1). Spherical tumor with a radius of 1.5 cm was established. The center of the tumor was at a depth of 4.5 cm. The boron concentrations in the soft tissue and tumor were 10 and 35 ppm, respectively. The boron concentration of the tumor/normal tissue ratio (T/N ratio) was constantly set at 3.5 for all boron concentration changes. We set the y-z plane in 1.5 cm deep of the phantom to score the quantities of interest, such as the number of Cherenkov photons and dose deposition.

To explore the availability of monitoring neutron beam through Cherenkov photons emission, we further simulated the morphology of a female breast tumor treated with BNCT based on the CHRP. Fig. 2 shows the CHRP geometry and beam setup in the simulation. CHRP was developed by our group based on Anatonium™ 3D P1 V5.0, which can represent Chinese physiological features (Geng et al., 2014). Based on the CHRP, a spherical tumor at 3.8 cm deep with 1.5 cm radius was established in the breast. CHRP was transformed into a voxel-based

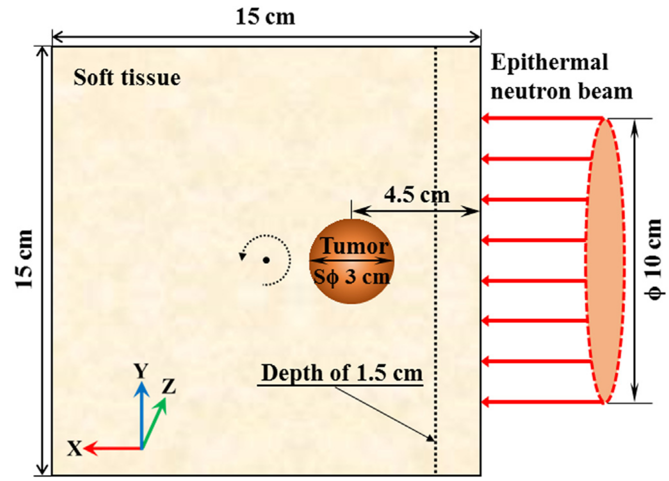

Fig. 1. Schematic of cubic phantom and beam setup in Geant4.

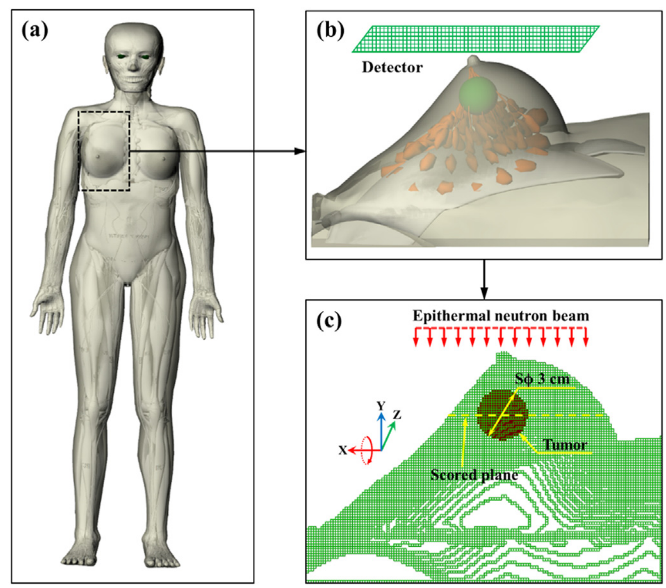

Fig. 2. Schematic of geometry and beam setup for CHRP containing breast tumor treated with BNCT.

model before importing into Geant4. The resolution of the model is $1.44 \times 1.44 \times 1.44\ mm^3$. The boron concentrations in tumor, skin, and healthy tissues were 35, 15, and 10 ppm, respectively. The scored plane was defined at 1.5 cm deep, as shown in Fig. 2(c). An array detector with $15 \times 15\ cm^2$ area was established 1.6 cm above the breast to detect the Cherenkov photons escaping from the skin surface, as shown in Fig. 2(b). The center of detector is located directly above the center of the tumor. The resolution of the detector is $0.25 \times 0.25\ cm^2$, and only Cherenkov photons can be scored. For the preliminary study of this novel method, we adopted a simplified setting of the detector, which will not affect the conclusion.

2.2. Neutron source

As shown in Fig. 1 and Fig. 2, epithermal neutron beam with the radius of 5 cm was employed to perpendicularly irradiate the two phantoms. The center of the tumor is on the central axis of the neutron beam. The energy spectrum shown as the black curve in Fig. 3, which was named "Neuboron", was obtained from an accelerator-based BNCT facility, which is currently under construction by Neuboron Medtech Ltd. in China (Lee et al., 2014). For this facility, neutrons are produced

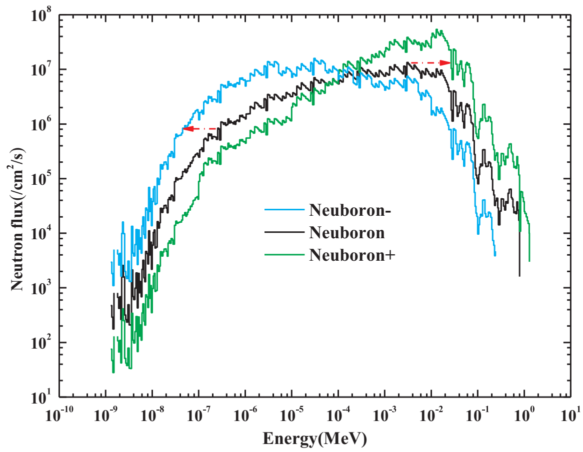

Fig. 3. Energy spectra of epithermal neutron beam used in simulation (Lee et al., 2014).

through the reaction of 2.5 MeV protons and 93.1 mm thick lithium target; and a beam shaping assembly (BSA) was designed to meet the free beam requirements of the International Atomic Energy Agency (IAEA).

In order to explore the relationship between the distribution of Cherenkov photons and the characteristics of the neutron beam, we intentionally changed the energy spectrum and neutron beam field orientation. The changes in the energy spectrum were achieved by shifting the original spectrum into the low-energy region (Neuboron-) and high-energy region (Neuboron+), as shown in Fig. 3. In clinical practice, the set-up error of the patient may change the relative position and neutron beam incidence direction. In this study, we considered this change as the inaccuracy of the neutron beam field orientation. The changes in the neutron beam field orientation were achieved by clockwise rotation of the cubic phantom (around the Z axis) and CHRP (around the X axis). The irradiation angles were 5, 10, and 15 degrees relative to the original beam orientation. Furthermore, all simulations were performed with 1.0×10^9 primary neutron particles to keep the statistical uncertainty below 2% for the results, and all results were normalized to one neutron.

3. Results

3.1. Tentative exploration based on the cubic phantom

3.1.1. Variations of BNCT dose distribution with varied neutron beam characteristics

In this section, the BNCT dose distribution influenced by the energy spectrum and the neutron beam field orientation was investigated. We calculated the radial distribution of BNCT dose under different neutron beam characteristics at 1.5 cm depth, as shown in Fig. 4.

In Fig. 4(a), the dose along the radial axis increased after shifting the original spectrum into the Neuboron-, and conversely the dose decreased when the Neuboron+ spectrum was used. The maximum relative variation of dose is 19.94%, compared with the results of the original Neuboron spectrum. The higher proportion of thermal neutrons in the energy spectrum, the greater BNCT dose will be, because the main contribution of dose comes from the capture reaction of thermal neutron in this depth. Fig. 4(b) shows the radial dose distribution when the neutron beam field orientation changes. With the increase of the irradiation angle, the maximum dose point is gradually shifted to the -Y axis direction, and the neutron beam deposits more dose in the -Y axis region. The maximum relative variation of dose is 78.14% compared with the results of neutron beam field orientation without change.

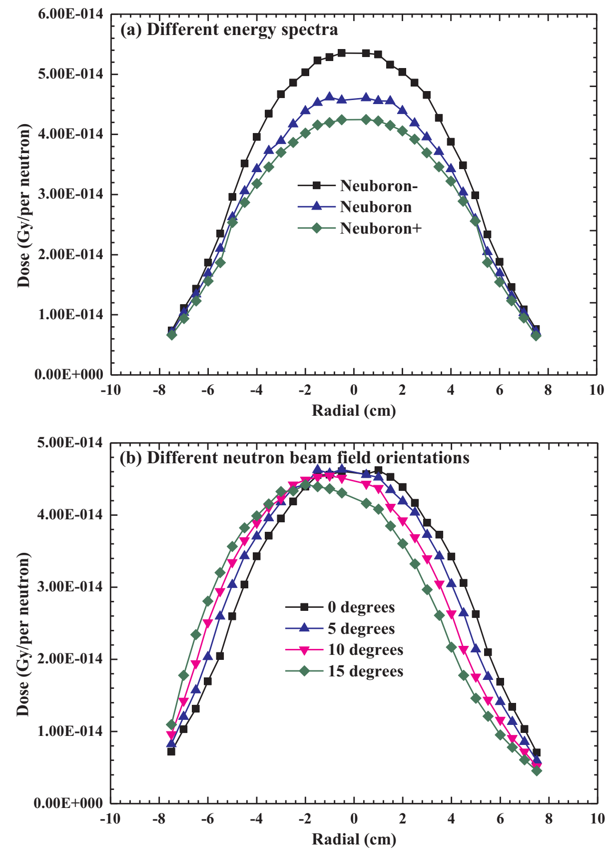

Fig. 4. Radial distribution of BNCT dose under different energy spectra and neutron beam field orientations.

3.1.2. Changes of distribution of Cherenkov photons in BNCT

Gamma rays generated in BNCT mainly come from the neutron capture reaction of neutrons with elements in the tissue. In this study, the production rates of gamma rays at 1.5 cm depth of the cubic phantom are shown in Table 1. The dose deposition of gamma rays is closely related to the characteristics of the neutron beam. In BNCT, the secondary-charged particles of gamma rays are the only source to generate Cherenkov photons. Therefore, the Cherenkov photons in the tissue should also be changed with the characteristics of the neutron beam and may have potential application for monitoring neutron beam. Thus, we explored the changes of Cherenkov photons and gamma dose as the neutron beam characteristic changes in BNCT. The radial distributions of Cherenkov photons and gamma dose on the scored plane were then calculated. All the results were normalized to the individual maximum value of Cherenkov photons and gamma dose.

Fig. 5 compares the radial distributions of Cherenkov photons with gamma dose under different neutron beam characteristics. The radial distributions of the Cherenkov photons and gamma dose almost coincided for a certain condition of boron distribution, indicating a favorable response relationship between the Cherenkov photons and gamma dose. Moreover, the distribution of Cherenkov photons changed with a different neutron beam configuration. The maximum relative difference in the number of Cherenkov photons reached 14.75% for the Neuboron- spectrum compared with the Neuboron spectrum. For the changes to the neutron beam field orientation, the maximum difference reached 14.68% when the incident direction was rotated at 5 degrees. However, the changes of Cherenkov photons caused by neutron spectrum and neutron beam field orientation are different, the change of neutron beam field will cause a radial shift in the distribution of Cherenkov photons.

In order to study the influence of other factors on the Cherenkov photons, we still need to investigate whether the changes of boron

Table 1
Production rates of gamma rays generated from neutron capture reaction at 1.5 cm depth.

Element	^{1}H	^{10}B	^{16}O	^{12}C	^{14}N	^{35}Cl	other	Total
E_{γ} (MeV)	2.223	0.478	1.088	1.262	1.885	1.165		
Production rate (kg^{-1}/neutron)	0.450	0.024	0.00015	0.00038	0.00046	0.00919	0.144	0.628

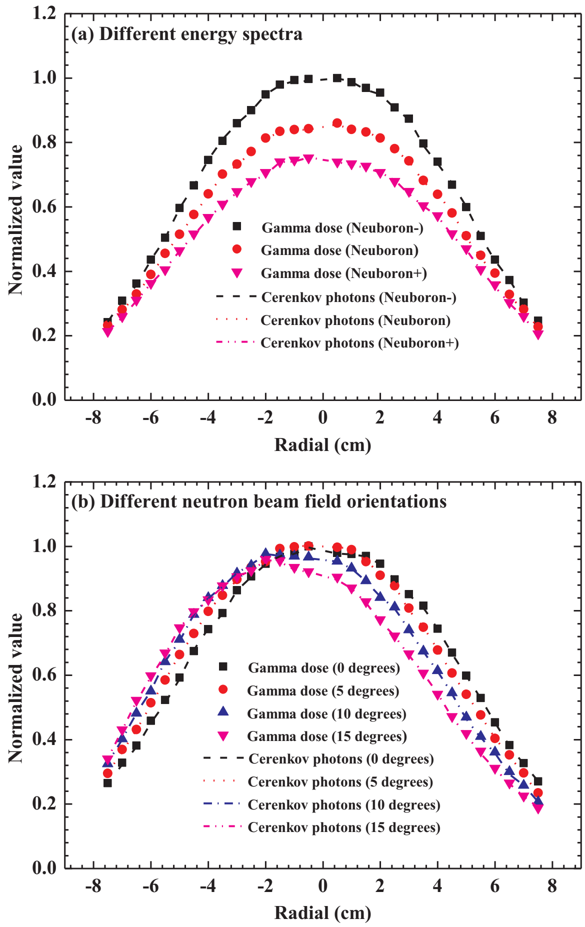

Fig. 5. Distributions of Cherenkov photons and gamma dose under different energy spectra and neutron beam field orientations.

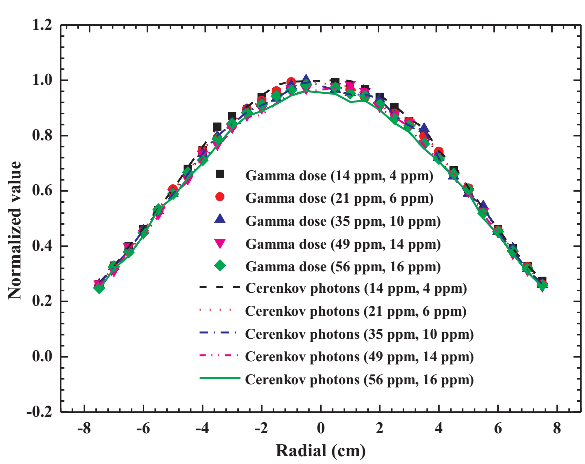

Fig. 6. Distributions of Cherenkov photons and gamma dose under different boron concentration distributions.

concentration distribution will lead to the changes in Cherenkov photons. Thus, the radial distributions of Cherenkov photons and gamma dose were obtained under different boron concentration distributions. As shown in Fig. 6, a favorable correlation between Cherenkov photons and gamma dose was observed under different boron concentration distributions. Nevertheless, the number of Cherenkov photons has a slight decrease with the increase of boron concentration, whereas the gamma dose is essentially constant. The decrease of Cherenkov photons is due to that the decrease of Cherenkov photons generated by secondary charged particles of 2.223 MeV gamma rays is larger than the increase of Cherenkov photons generated by secondary charged particles of 0.478 MeV gamma rays. Consequently, a certain degree of deviation was noted between the distribution of Cherenkov photons and gamma dose. However, the maximum relative deviation of Cherenkov photons is within 3.51%, even if the relative change in boron concentration reaching 60%.

3.1.3. Changes of 2D distribution of Cherenkov photons with different neutron beam characteristics

The 2D distribution of Cherenkov photons enables us to intuitively observe their changes in the phantom. Thus, we calculated the Cherenkov photons generated on the scored plane with different neutron beam characteristics to further explore the feasibility of using Cherenkov photons for monitoring neutron beam in BNCT. The unit of Cherenkov photons is defined as the number of Cherenkov photons generated in a unit mass of medium when the incident particle is one neutron.

Fig. 7 shows the changes of 2D distribution of Cherenkov photons for neutron beams with different energy spectra. As the proportion of high-energy neutrons in the spectrum increases, the number of Cherenkov photons gradually decreases. This is due to the smaller cross section of high-energy neutron for the capture reaction with hydrogen or boron, resulting in the reduction of gamma rays. However, the number of Cherenkov photons in the central area is also stronger than that in the surrounding area. The maximum intensity of Cherenkov photons for three kinds of energy spectra are 36.30, 31.11, and 27.19 kg^{-1} per neutron, respectively. For the different neutron beam field orientations, the maximum number of Cherenkov photons has a slight decline with the increase of irradiation angle, as shown in Fig. 8. The more noticeable phenomenon is that the high-intensity region of Cherenkov photons shifts gradually toward the -Y axis.

3.2. Potential application study based on CHRP

3.2.1. 2D distributions of Cherenkov photons and gamma dose for different neutron beam characteristics

In the previous sections, the validity of using Cherenkov photons for real-time monitoring of neutron beam was preliminarily demonstrated based on a cubic phantom. To further simulate a clinical scenario, CHRP was used to investigate this method in a more realistic situation. For a constant boron concentration distribution, changes in the 2D distribution of Cherenkov photons on the scored plane with different neutron beam characteristics are shown in Fig. 9 and Fig. 10. Meanwhile, as the change of Cherenkov photons was completely caused by the change in gamma dose deposition, we compared the gamma dose distribution with the Cherenkov photons distribution.

As shown in Fig. 9, the center of the high-intensity region is not at the center of the tumor (X = −1.08, Z = −3.456), which is due to the

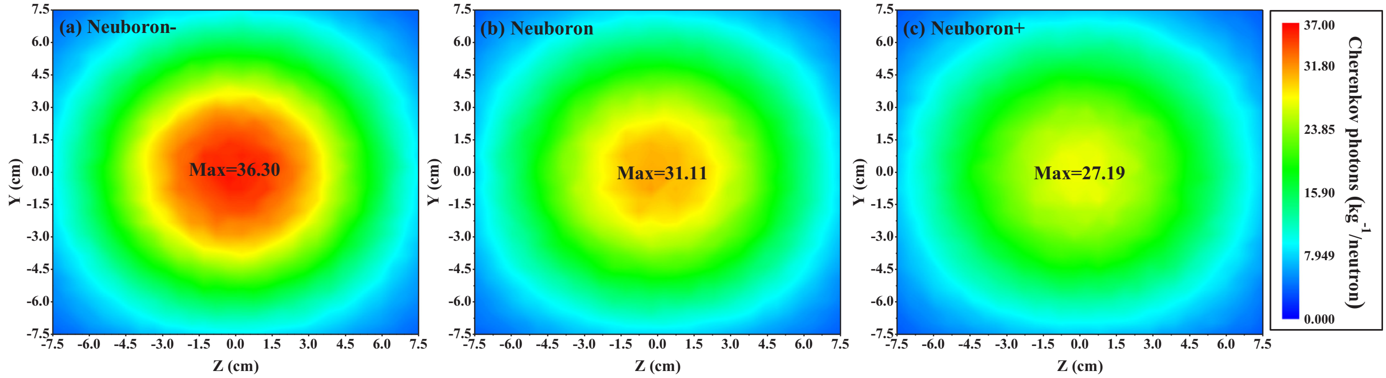

Fig. 7. 2D distributions of Cherenkov photons on the scored plane for neutron beams with different energy spectra.

different thicknesses of tissue between the scored plane and the skin surface. Similar to the results observed from the cubic phantom, the number of Cherenkov photons decreases when the spectrum shifts to Neuboron + . Compared with the result of the neutron beam with the Neuboron spectrum, the relative variations of the maximum number of Cherenkov photons are 11.86% and 14.26% for Neuboron- and Neuboron + spectra, respectively. Fig. 10 shows the changes in the distribution of Cherenkov photons for different neutron beam field orientations. The red lines approximately represent that the number of Cherenkov photons in those positions above 75% of the maximum number of Cherenkov photons. In this case, the high-intensity region of Cherenkov photons gradually shifts toward the Z axis with the increase of irradiation angle.

In order to quantitatively analyze the changes in the intensity and distribution of Cherenkov photons, we obtained the 1D distribution of Cherenkov photons at X = −1.73 cm, as shown in Fig. 11. Obviously, the intensity of Cherenkov photons varies with the neutron energy spectrum. For different neutron beam field orientations, we chose the Z-axis value corresponding to 75% of Cherenkov photons maximum value to quantify the shift of Cherenkov photons distribution. The shift values are 0.53 cm, 0.70 cm, and 0.84 cm with the increasing change of neutron beam field orientation, respectively. Besides, the relative variations of the number of Cherenkov photons were obtained, as shown in Fig. 12. The proportions of relative variation more than 10% with the increasing irradiation angle were 39.72%, 44.39%, and 51.31%, respectively. Furthermore, a significant consistency between the distribution of gamma dose and Cherenkov photons was observed regardless of the changes in energy spectrum or neutron beam field orientation.

3.2.2. Detection of Cherenkov photons with different neutron beam characteristics

Although the characteristics of neutron beam can indeed lead to the changes in Cherenkov photons distribution inside a phantom, in order to demonstrate the practical application, we propose to use a flat array detector to detect Cherenkov photon distribution. The setting of the

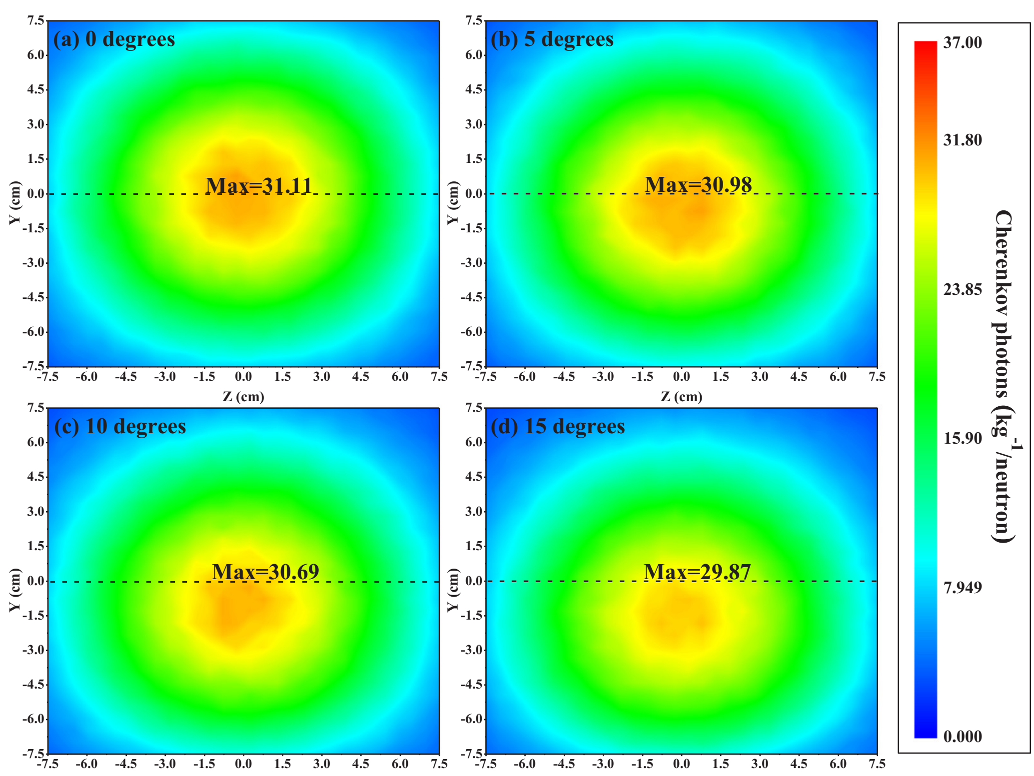

Fig. 8. 2D distributions of Cherenkov photons on the scored plane for different neutron beam field orientations.

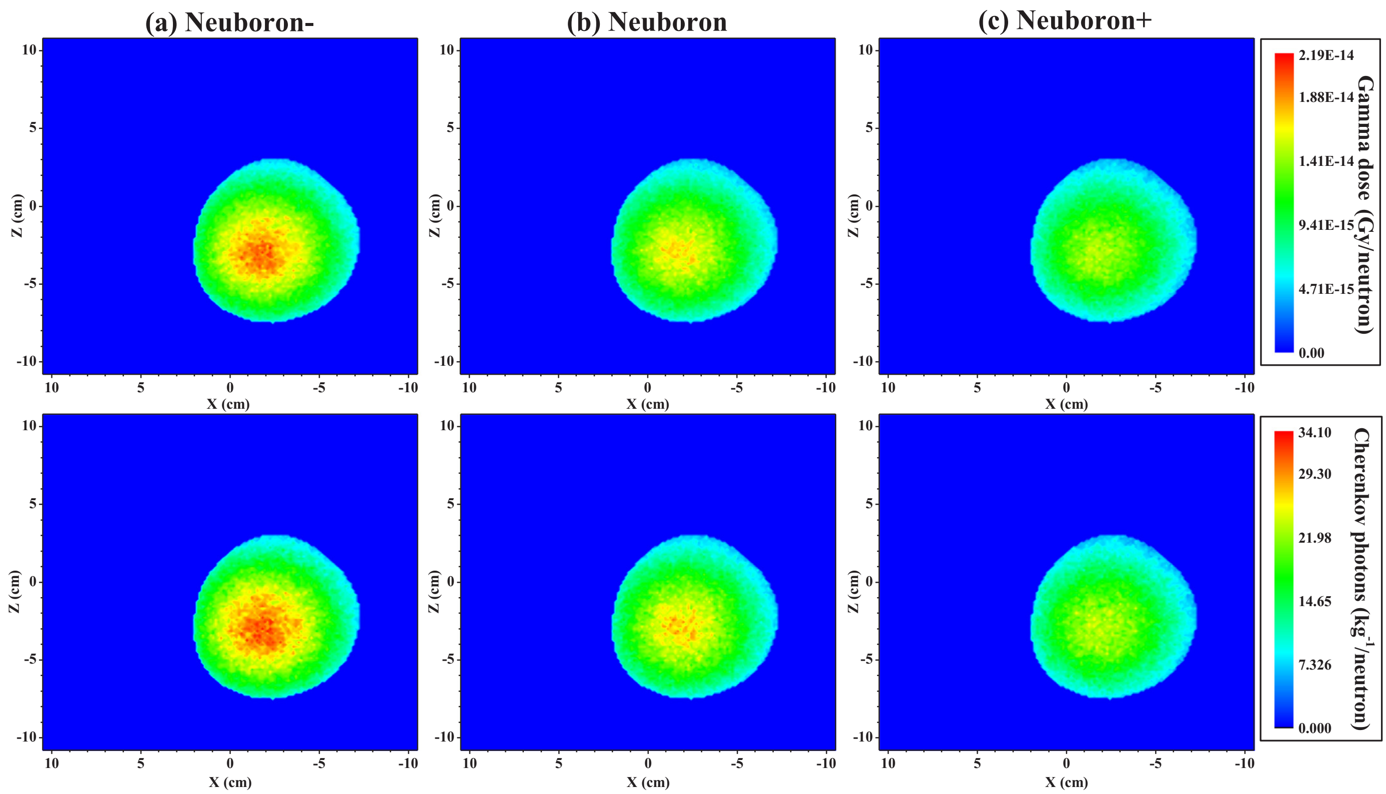

Fig. 9. 2D distributions of gamma dose and Cherenkov photons on the scored plane for neutron beams with different energy spectra.

detector has been shown in Section 2.1. The distributions of Cherenkov photons reaching the detector array were scored for different neutron beam characteristics (see Fig. 13 and Fig. 14).

Because of the poor penetrability of Cherenkov photons in the tissue, only the Cherenkov photons originating from superficial tissue where the depth is approximately less than 0.5 cm can be detected. Distribution of Cherenkov photons reaching the detector should be similar to the distribution of Cherenkov photons generated in the

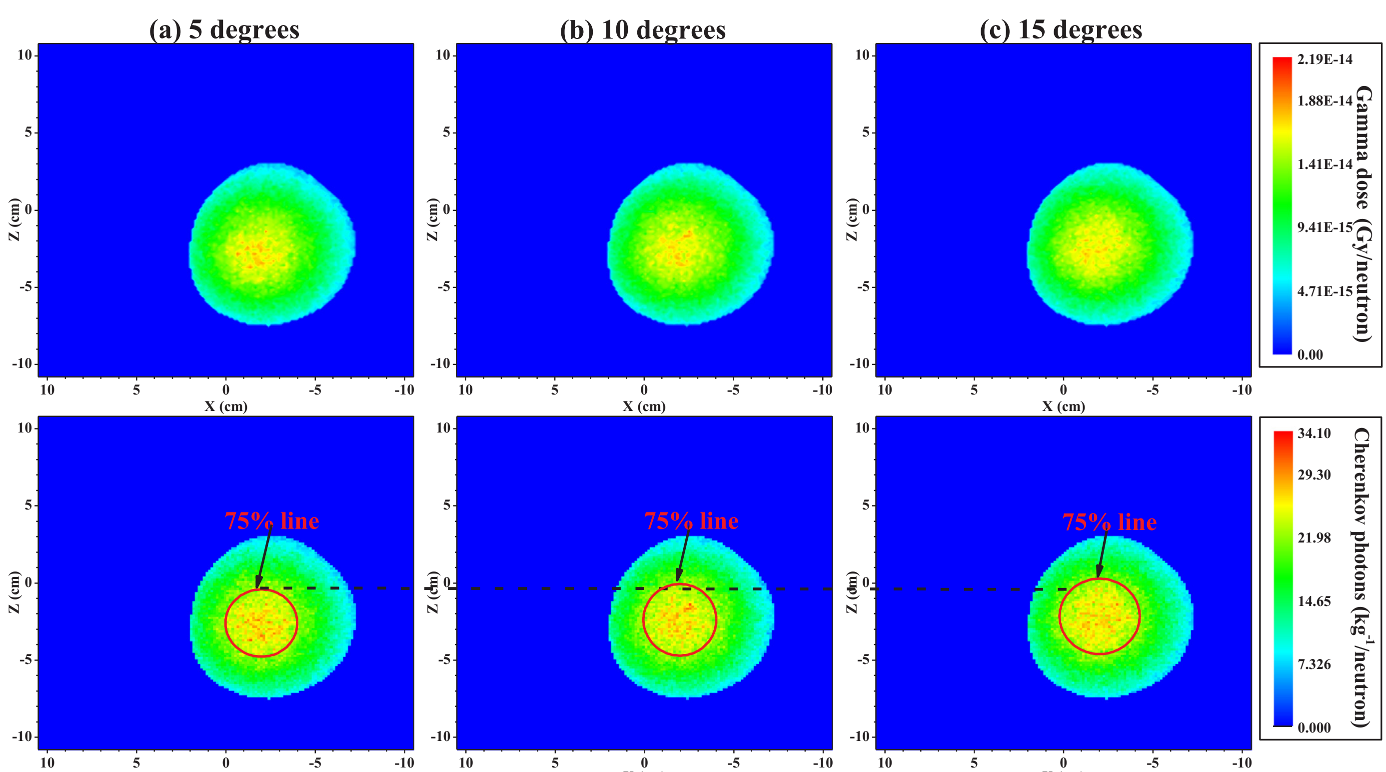

Fig. 10. 2D distributions of gamma dose and Cherenkov photons on the scored plane for different neutron beam field orientations.

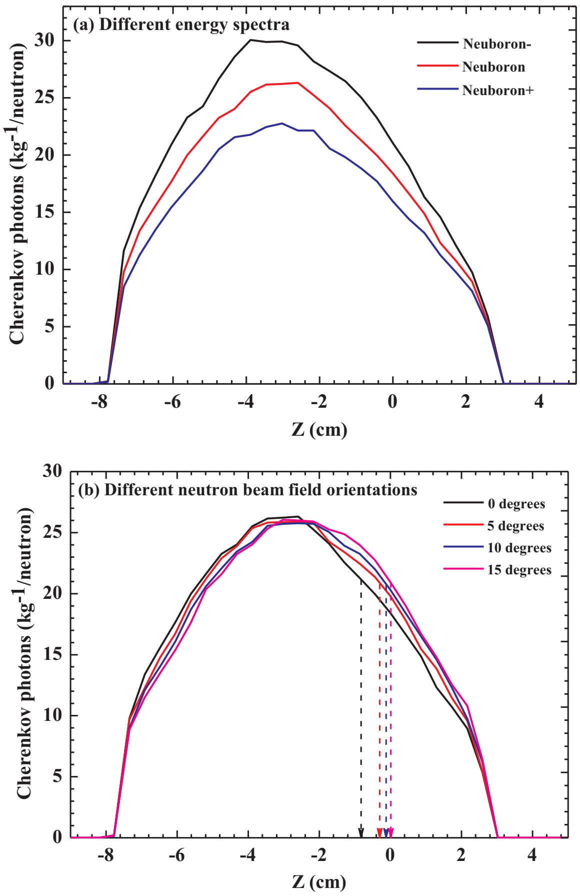

Fig. 11. 1D distributions of Cherenkov photons at X = −1.73 cm under different energy spectra and neutron beam field orientations.

superficial tissue. As shown in Fig. 13, the distributions of Cherenkov photons changes for different neutron energy spectra. The maximum numbers of Cherenkov photons for Neuboron-, Neuboron and Neuboron + spectra are 3.67E-06, 3.08E-06 and 2.61E-06 per neutron, respectively. Fig. 14 shows the distributions of Cherenkov photons scored by detector array for different neutron beam field orientations. In this case, the relative position between the detection array and the phantom was changed, and the position and size of the region containing the highest intensity Cherenkov photons apparently changed. Comparing with the distribution of Cherenkov photons for initial neutron beam characteristic, the relative variations of Cherenkov photons for different neutron beam field orientations were shown in Fig. 15. The proportions of relative variation more than 10% with the increasing irradiation angle were 7.28%, 19.69%, and 27.19%, respectively.

4. Discussion

The neutron beam characteristic is one of the key factors determining the dose in BNCT. We also demonstrate that the variation of neutron spectrum and neutron beam field orientation can largely affect the BNCT dose delivery (Fig. 4). Thus, it is necessary to continuously develop new methods for monitoring the neutron beam. In this study, the results based on the cubic phantom and CHRP show that the Cherenkov photons changes with neutron spectrum and neutron beam field orientation (Fig. 5, Figs. 7–10), which make it possible to use Cherenkov photons for neutron beam monitoring. The change in boron concentration can also cause the change in Cherenkov photons intensity (Fig. 6). However, the change of boron concentration will be relatively small by using several quality control methods during neutron irradiation (Kiger et al., 2004; Koivunoro et al., 2015). The change of Cherenkov photons caused by boron concentration is minimal. Therefore, only the neutron beam characteristics can lead to significant change in Cherenkov photons.

Actually, the change of neutron spectrum will only result in the change of Cherenkov photons intensity, and the change of neutron beam field orientation will cause a shift in the distribution of Cherenkov photons (Figs. 9–10). Therefore, we can distinguish whether the neutron spectrum or neutron beam field orientation has changed through monitoring of both the intensity and the distribution of Cherenkov photons. The greater the variation of Cherenkov photons, the greater the variation of neutron beam characteristic relative to the initial characteristic will be. Besides, the degree of change in Cherenkov photons caused by neutron beam characteristic is different at different depths of the phantom. For the change in energy spectrum, the change of Cherenkov photons is possible to be relatively large in the shallow depths (< 0.5 cm). Because the difference in the neutron spectrum becomes smaller with the increase in depth. For changes of the neutron beam field orientation, the change of Cherenkov photons in different depths needs to be further explored. However, the change of Cherenkov photons at shallow depth should be focused on, because only the Cherenkov photons generated in this region can be detected. Furthermore, the different geometrical morphologies of tissue, where it is irradiated by neutron beam, also affects the variation degree of Cherenkov photons.

Overall, the monitoring of neutron beam field orientation could be easily realized through the distribution of Cherenkov photons detection. But both the change of boron concentration and neutron beam spectrum only result in the change of Cherenkov photons intensity, and the changes are similar. We can confirm that the neutron beam spectrum has changed when the intensity of Cherenkov photons is significantly changed. However, determining on whether the change is caused by boron concentration or by neutron beam spectrum is difficult when the intensity of Cherenkov photons has extremely minimal change. The maximum relative variation of Cherenkov photons in the detector array caused by the change in boron concentration needs to be

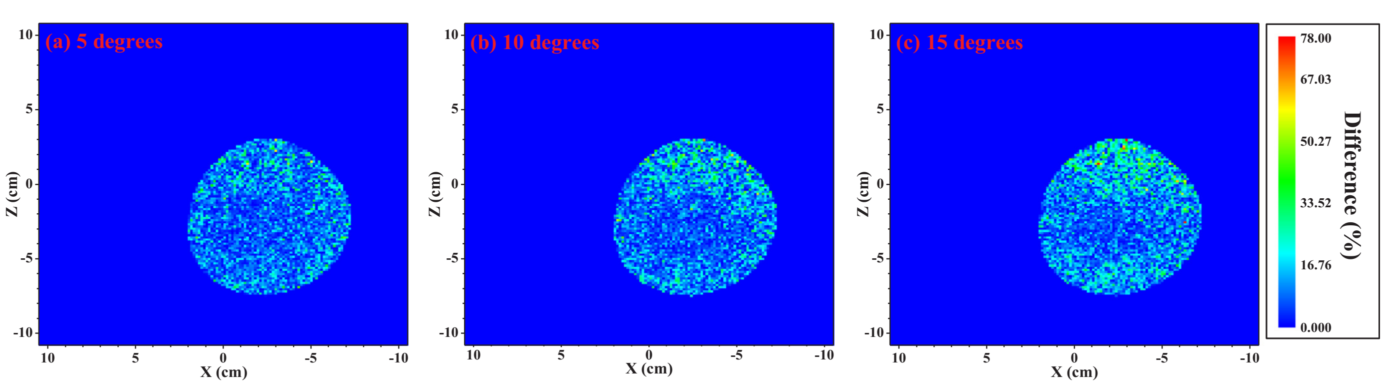

Fig. 12. Relative variation of Cherenkov photons for different neutron beam field orientations.

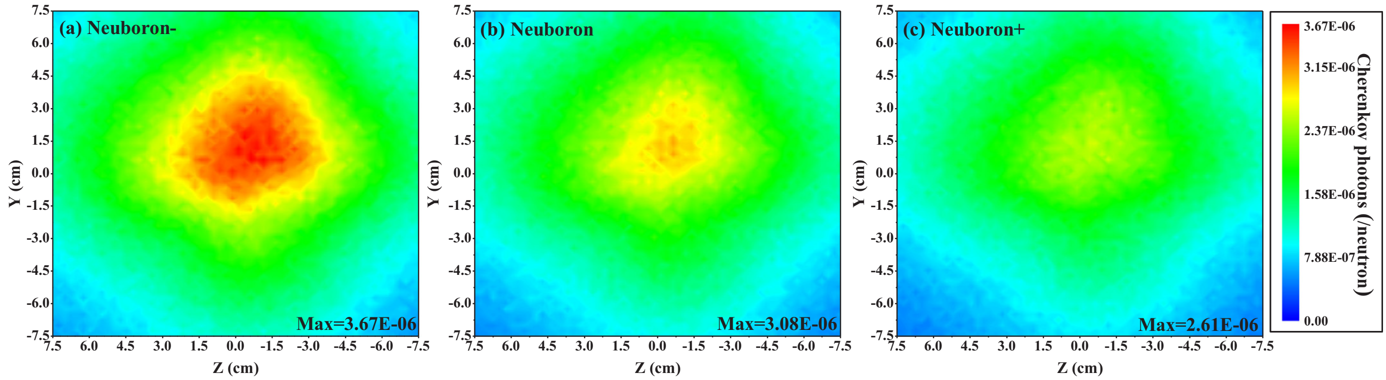

Fig. 13. Number of Cherenkov photons scored by detector array for different energy spectra of neutron beam.

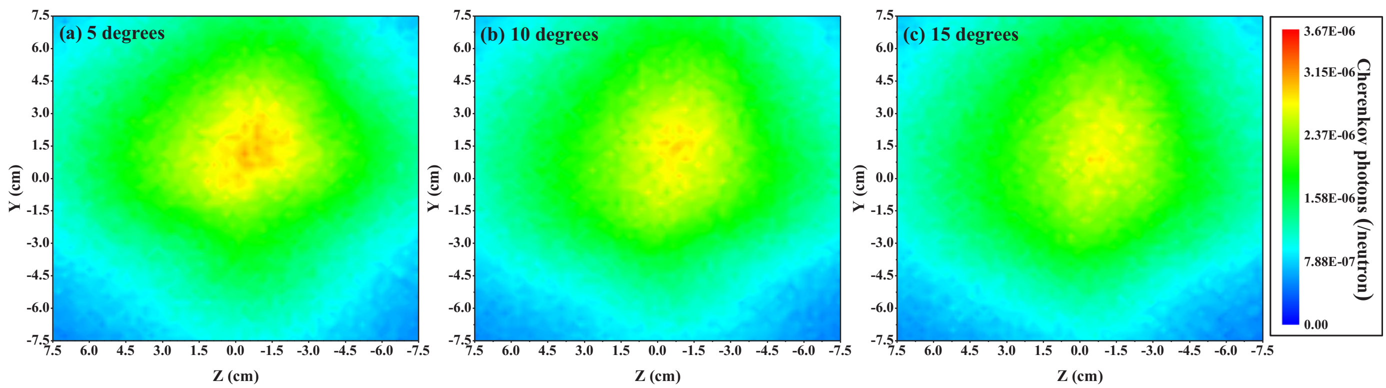

Fig. 14. Number of Cherenkov photons scored by detector array for different neutron beam field orientations.

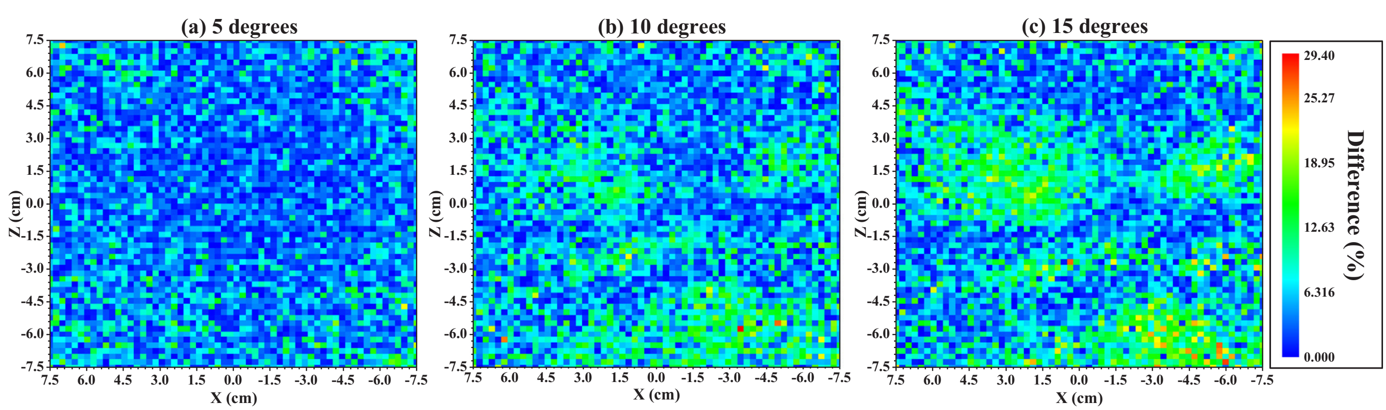

Fig. 15. Relative variation of Cherenkov photons identified by a detector array for different neutron beam field orientations.

further investigated. Otherwise, we need to find a method to distinguish the difference between the changes of Cherenkov photons caused by boron concentration and caused by neutron beam spectrum. Nonetheless, the change of Cherenkov photons suggests that the dose in the skin has changed at least. Furthermore, although we simulated the detection of Cherenkov photons with different neutron beam characteristics (Figs. 13–14), our group will experimentally test this method in BNCT with an electron multiplying charge-coupled device (EMCCD). In practical experiment, gamma rays will generate noise in the detector, and it is necessary to reduce the noise as much as possible by means of high-transparency shielding material and image processing algorithm, which needs to be further studied in the future.

5. Conclusions

In this study, a cubic phantom and CHRP were used to investigate the real-time monitoring method on the neutron beam by using Cherenkov photons in BNCT. Based on the cubic phantom, we first demonstrated that the dose distribution is affected by neutron beam characteristics in BNCT. The maximum relative variation of dose are 19.94% and 78.14% when the usage of neutron beam with Neuboron- spectrum and neutron beam field orientation with 15 degrees change, respectively. Then, the favorable response relationship between Cherenkov photons and gamma dose was existed on the scored plane. More importantly, the number of Cherenkov photons changes with the neutron energy spectrum, and the maximum relative variation in the number of Cherenkov photons was 14.75% for Neuboron- spectrum. Meanwhile, the radial shift in the distribution of Cherenkov photons caused by the change of neutron beam field orientation was observed, which leads a maximum relative variation of 14.68% in the number of Cherenkov photons for 5 degrees change of neutron beam field orientation. Those changes were more intuitively demonstrated by the 2D distribution of Cherenkov photons. However, only 3.51% of the maximum change of Cherenkov photons occurred when the relative change of boron concentration reaches 60%. In fact, the change of Cherenkov photons due to the variation of boron distribution was relatively small during the treatment. Thus, we approximately consider that the significant change of Cherenkov photons can only be caused by neutron beam characteristics. Furthermore, the changes of Cherenkov photons for different neutron beam characteristics were also observed in the CHRP, and they are detectable through the detector outside the phantom. In particular, even for the results of detection, the proportions of relative variation more than 10% with the increasing change of neutron beam field orientation in the detection image were 7.28%, 19.69%, and 27.19%, respectively. Those changes are obvious, which can be used to realize the real-time monitoring of neutron beam. In practice, we can predict a expect distribution and intensity of Cherenkov photons, and then detect the corresponding distribution during therapy to monitoring the stability of the irradiating neutron beam.

Acknowledgments

This work was supported by the National Natural Science Foundation of China (Grant No. 11475087); the National Key Research and Development Program (Grant No. 2017YFC0107700); the National Key Research and Development Program (Grant No. 2016YFE0103600); the Funding of Postgraduate Research & Practice Innovation Program of Jiangsu Province (Grant No. KYLX16_0351); and the Priority Academic Program Development of Jiangsu Higher Education Institutions.

References

Agostinelli, S., Allison, J., Amako, K., et al., 2003. GEANT4—a simulation toolkit. Nucl. Instrum. Methods A 506, 250–303.

Auterinen, I., Serén, T., Kotiluoto, P., Uusi-Simola, J., Savolainen, S., 2004. Quality assurance procedures for the neutron beam monitors at the FiR 1 BNCT facility. Appl. Radiat. Isot. 61, 1015–1019.

Bashkatov, A.N., Genina, E.A., Tuchin, V.V., 2011. Optical properties of skin, subcutaneous, and muscle tissues: a review. J. Innov. Opt. Health Sci. 4, 9–38.

Blue, T.E., Yanch, J.C., 2003. Accelerator-based epithermal neutron sources for boron neutron capture therapy of brain tumors. J. Neuro-Oncol. 62, 19–31.

Cherenkov, P.A., 1934. Visible emission of clean liquids by action of γ radiation. Dokl. Akad. Nauk SSSR 2, 451.

Geng, C.R., Tang, X.B., Hou, X.X., Shu, D.Y., Chen, D., 2014. Development of Chinese hybrid radiation adult phantoms and their application to external dosimetry. Sci. China Technol. Sci. 57, 713–719.

Green, S., 1998. Developments in accelerator based boron neutron capture therapy. Radiat. Phys. Chem. 51, 561–569.

Helo, Y., Rosenberg, I., D'Souza, D., MacDonald, L., Speller, R., Royle, G., Gibson, A., 2014a. Imaging Cerenkov emission as a quality assurance tool in electron radiotherapy. Phys. Med. Biol. 59, 1963–1978.

Helo, Y., Kacperek, A., Rosenberg, I., Royle, G., Gibson, A.P., 2014b. The physics of Cerenkov light production during proton therapy. Phys. Med. Biol. 59, 7107–7123.

Kiger, W.S., Lu, X.Q., Harling, O.K., Riley, K.J., Binns, P.J., Kaplan, J., Patel, H., Zamenhof, R.G., Shibata, Y., Kaplan, I.D., Busse, P.M., Palmer, M.R., 2004. Preliminary treatment planning and dosimetry for a clinical trial of neutron capture therapy using a fission converter epithermal neutron beam. Appl. Radiat. Isot. 61, 1075–1081.

Koivunoro, H., Hippeläinen, E., Auterinen, I., Kankaanranta, L., Kulvik, M., Laakso, J., Seppala, T., Savolainen, S., Joensuu, H., 2015. Biokinetic analysis of tissue boron (B-10) concentrations of glioma patients treated with BNCT in Finland. Appl. Radiat. Isot. 106, 189–194.

Lee, P.Y., Liu, Y.H., Jiang, S.H., 2014. Dosimetric performance evaluation regarding proton beam incident angles of a lithium-based AB-BNCT design. Radiat. Prot. Dosim. 161, 403–409.

Moss, R.L., 2014. Critical review, with an optimistic outlook, on Boron Neutron Capture Therapy (BNCT). Appl. Radiat. Isot. 88, 2–11.

Nigg, D.W., Wemple, C.A., Venhuizen, J.R., Tripard, G.E., Sharp-Dugan, S., Fox, K., Gavin, P.R., 2002. Preliminary neutronic performance assessment of an epithermal neutron beam for preclinical BNCT research at Washington state University. INEEL Adv. Radiother. Res. Prog. Annu. Rep. 2001. pp. 35–50.

Palmer, M.R., Goorley, J.T., Kiger, W.S., Busse, P.M., Riley, K.J., Harling, O.K., Zamenhof, R.G., 2002. Treatment planning and dosimetry for the Harvard-mit phase I clinical trial of cranial neutron capture therapy. Int. J. Radiat. Oncol. 53, 1361–1379.

Perks, C.A., Mill, A.J., Constantine, G., Harrison, K.G., Gibson, J.A., 1988. A review of boron neutron capture therapy (BNCT) and the design and dosimetry of a high-intensity, 24 keV, neutron beam for BNCT research. Br. J. Radiol. 61, 1115–1126.

Probst, T.U., 1999. Methods for boron analysis in boron neutron capture therapy (BNCT). A review. Fresenius J. Anal. Chem. 364, 391–403.

Raaijmakers, C.P., Nottelman, E.L., Konijnenberg, M.W., Mijnheer, B.J., 1996. Dose monitoring for boron neutron capture therapy using a reactor-based epithermal neutron beam. Phys. Med. Biol. 41, 2789–2797.

Shu, D.Y., Tang, X.B., Geng, C.R., Gong, C.H., Chen, D., 2016. Determination of the relationship between dose deposition and Cerenkov photons in homogeneous and heterogeneous phantoms during radiotherapy using Monte Carlo method. J. Radioanal. Nucl. Chem. 308, 187–193.

Silva, I., Pang, G., 2012. Characteristics of radiation induced light in optical fibres for portal imaging application. Radiat. Phys. Chem. 81, 599–608.

Tanner, V., Auterinen, I., Helin, J., Kosunenb, A., Savolainenc, S., 1999. On-line neutron beam monitoring of the Finnish BNCT facility. Nucl. Instrum. Methods A. 422, 101–105.

Verbakel, W.F.A.R., Stecher-Rasmussen, F., 1997. A γ-ray telescope for on-line measurements of low boron concentrations in a head phantom for BNCT. Nucl. Instrum. Methods A 394, 163–172.

Wittig, A., Michel, J., Moss, R.L., Stecher-Rasmussen, F., Arlinghaus, H.F., Bendel, P., Mauri, P.L., Altieri, S., Hilger, R., Salvadori, P.A., Menichetti, L., Zamenhof, R., Sauerwein, W.A.G., 2008. Boron analysis and boron imaging in biological materials for boron neutron capture therapy (BNCT). Crit. Rev. Oncol. Hematol. 68, 66–90.

Zhang, R., Andreozzi, J.M., Gladstone, D.J., Hitchcock, W.L., Glaser, A.K., Jiang, S.D., Pogue, B.W., Jarvis, L.A., 2014. Cherenkoscopy based patient positioning validation and movement tracking during post-lumpectomy whole breast radiation therapy. Phys. Med. Biol. 60, L1–L14.